

# Design of a Novel High-Gain Dual-Band Antenna for WLAN Applications

Xiaoxiang He, Sheng Hong, *Student Member, IEEE*, Huagang Xiong, Qishan Zhang, *Senior Member, IEEE*, and Emmanouil Manos M. Tentzeris, *Senior Member, IEEE*

**Abstract**—A novel high-gain, dual-band antenna covering IEEE 802.11a/b/g bands is presented in this letter for wireless local area network (WLAN) applications. The antenna is composed of a fork-like monopole, a rectangular ring, and a miniaturized rectangular patch. The backside radiation of the antenna is effectively reflected back by a rectangular metal, so maximum gain with the values of 6.2 and 10.4 dBi are achieved in the lower and higher frequency band, respectively. The return loss, radiation pattern, and the critical design parameters are also investigated in detail. Simulated and measured results verify that the presented antenna is a good solution for dual-band WLAN long-distance communication applications.

**Index Terms**—Antenna gain, antennas, multiple-band antenna, wireless local area network (WLAN).

## I. INTRODUCTION

THE wireless local area networks (WLANs) working at 2.4- and/or 5.8-GHz bands have become almost ubiquitous with ever-increasing market penetration [1]. The operating frequencies cover, in the lower band (IEEE 802.11b/g), 2.4–2.48 GHz with 11/54-Mbps data rates, while in the higher frequency band (IEEE 802.11a), it is different from country to country. In the United States, the frequency ranges from 5.15–5.35 GHz and from 5.725–5.825 GHz, while in Europe, the frequency covers 5.15–5.35 GHz and 5.470–5.725 GHz, respectively. Nowadays, dual-band WLAN systems combining IEEE 802.11a/b/g standards are becoming more attractive [1]. A dual-band/wideband antenna is a key component for such communication systems [1]–[19], especially for “universal” applications, where it should be covering the whole 2.4–2.5-GHz and 5.15–5.85-GHz bands for dual-band WLAN. Such dual-band antennas with single feed have been proposed in various configurations [1], [5], [7], [8], [11], [13]. These antennas either provide inadequate coverage at the 5-GHz band [5], [7], [8], [11], or they cannot be easily integrated in

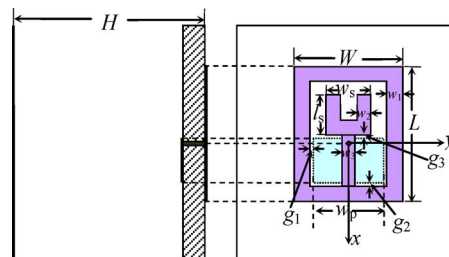


Fig. 1. Configuration of the proposed antenna.

TABLE I  
PARAMETERS OF THE PROPOSED ANTENNA (mm)

$L$	$W$	$L_s$	$w_s$	$w_p$	$H$
63.86	52.96	18.69	21.81	34.15	102.8
$g_1$	$g_2$	$g_3$	$w_1$	$w_2$	$w_3$
1.56	1.4	1.56	7.79	6.85	6.54

portable devices [1], [13]. Furthermore, the gains of previously published single-fed dual-band antennas are lower than 6 dBi [1]–[15], even for simple compact-element arrays [16]. The gains of the antennas proposed in [17]–[19] are much higher, but also less than 8 dBi. Those designed low-profile antennas are suitable for portable devices, but in applications such as long-range communications or point-to-point communications devices running on battery, high gain of WLAN antenna is necessary, and the antennas previously published have difficulty meeting the requirement.

In this letter, a single-fed dual-band antenna covering IEEE 802.11a/b/g for WLAN applications is presented. The maximum gains of the two bands are 6.2 and 10.4 dBi, respectively, making the proposed antenna appropriate for high-gain applications.

## II. ANTENNA DESIGN

The proposed antenna is shown in Fig. 1, and the detailed parameters are listed in Table I. Without loss of generality, the modeled antenna was fed with a 50- $\Omega$  coaxial and SMA connector and was printed on the FR4 substrate (with the dimension of 109.03 mm  $\times$  77.88 mm  $\times$  1.5 mm and the relative permittivity  $\epsilon_r = 3.5$ ). The radiator is composed of three parts: the fork-like monopole, the rectangular ring, and the rectangular patch. A metal reflector with the same dimensions as the substrate is used behind the designed antenna, so the directivity/gain of the presented antenna is enhanced for both bands by suppressing the backside radiation. However, the overall volume of

Manuscript received June 12, 2009. First published July 07, 2009; current version published July 28, 2009. This work was supported in part by the National Nature Science of China under Grant 60601024.

X. He is with Nanjing University of Aeronautics and Astronautics, Nanjing 210016, China (e-mail: eexxhe@nuaa.edu.cn).

S. Hong, H. Xiong, and Q. Zhang are with Beihang University, Beijing 100191, China (e-mail: Fengqiao1981@gmail.com; hgxiang@ee.buaa.edu.cn; zhangqishan@263.net).

E. M. M. Tentzeris is with the School of Electrical and Computer Engineering, Georgia Institute of Technology, Atlanta, GA 30332 USA (e-mail: etentze@ece.gatech.edu).

Color versions of one or more of the figures in this letter are available online at <http://ieeexplore.ieee.org>.

Digital Object Identifier 10.1109/LAWP.2009.2026495

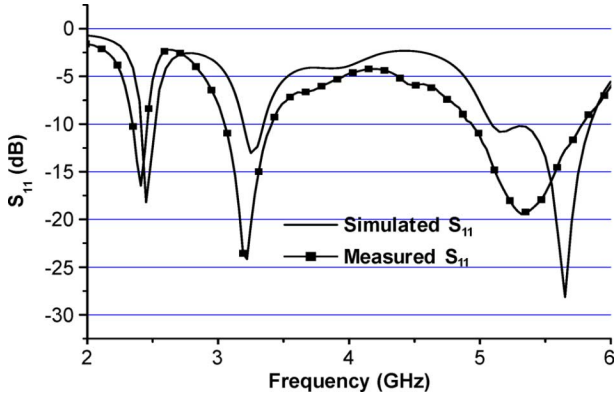


Fig. 2. The simulated and measured return loss.

the antenna (109.03 mm × 77.88 mm × 102.8 mm) is a bit larger than the antennas reported [1], [5], [7], [8], [11], [13]. The ring, together with the feed line, acts as a wideband impedance matching. The fork-like monopole resonates at two frequency points, with values ( $f^1, f^2$ ) that can be approximated as following [15]:

$$f^1 = \frac{c}{2L_1\sqrt{\epsilon_r}} \quad (1)$$

$$f^2 = \frac{c}{2L_2\sqrt{\epsilon_r}} \quad (2)$$

where

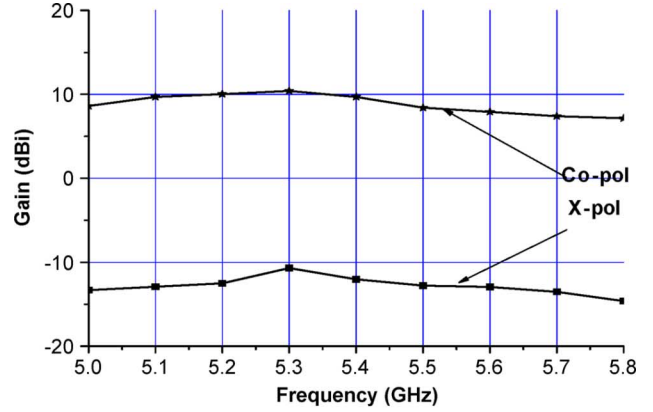
$$L_1 = L_s + (W_s - W_3)/2 \quad (3)$$

$$L_2 = (L_s - W_2) + (W_s - 2W_2 - W_3)/2. \quad (4)$$

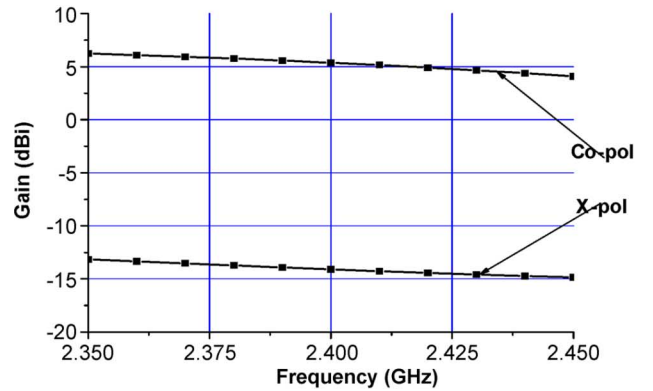
$L_1$  and  $L_2$  stand for the length of current trace operating at two frequency points along outside ( $L_1$ ) and inside ( $L_2$ ) of the monopole.  $c$  is the free-space velocity of light. Substituting the parameters in Table I to the formulations of (1) and (2), the oscillating frequency points of fork-like radiator are approximately equal to 3.045 and 6.39 GHz. The contribution of the miniaturized rectangular patch is to expand the high-frequency bandwidth of IEEE 802.11a with higher mode. All the parameters of the proposed antenna are optimized with Ansoft HFSS to fine-tune the theoretical values calculated above.

### III. EXPERIMENTAL RESULTS

To verify the high performance of the proposed antenna, return loss was simulated with Ansoft HFSS and measured with a vector network analyzer. As shown in Fig. 2, the measured and simulated results are in good agreement. The simulated and the experimental  $S_{11}$  below  $-10$ -dB bandwidths range from 2.4–2.52 GHz/2.35–2.45 GHz and from 5.1–5.85 GHz/4.94–5.79 GHz with the relative bandwidth 4.8%/4.2% and 13.7%/15.8%, respectively, which shows a minor frequency shift owing to fabrication variations and the loss of FR4 substrate. The IEEE 802.11b/g band is realized by the first resonant frequency of the fork-like monopole by formulation (1), and the IEEE802.11a band radiation field is contributed by the second frequency band of the monopole by formulation (2) together with the higher mode ( $TM_{12}$ ) of



(a)



(b)

Fig. 3. Measured gain in the two operating bands. (a) Measured gain in the lower frequency band; (b) measured gain of higher frequency band.

the rectangular patch. Between the two bands, there is another operating band from 3.04–3.42 GHz, which is formed by  $TM_{10}$  mode of the rectangular patch and is not taken into consideration in this letter, although it could be easily fine-tuned for WiMax applications.

The gain values of the antenna in the two bands were also measured, as shown in Fig. 3. In the higher frequency band, the copolarized maximum gain plotted in Fig. 3(a) is as large as 10.4 dBi, which is much higher than the gains of previously reported antennas. Because of the affect of higher mode of rectangular patch, the gain drops down between 5.4 and 5.8 GHz. The cross polarization in this band is below  $-10$  dBi, so the cross-polarization suppression is more than 20 dBi and is suitable for wireless applications. For the narrow lower band, the figure of gain versus frequency is also presented in Fig. 3(b), and the maximum gain of copolarization was measured to be 6.2 dBi with the cross polarization of 14.8 dBi in this band; thus, the cross-polarization suppression in this band is also more than 20 dBi. The higher gain in the higher frequency band can compensate for the higher propagation loss so that the two bands can cover almost the same communication area.

Curves in Figs. 4 and 5 show the experimental results of normalized radiation pattern in  $X$ - $Z$  plane and  $Y$ - $Z$  plane in the two bands. The maximum gain is not obtained at  $\theta = 0^\circ$  in  $X$ - $Z$  plane at 2.4 GHz due to the unsymmetrical structure in this

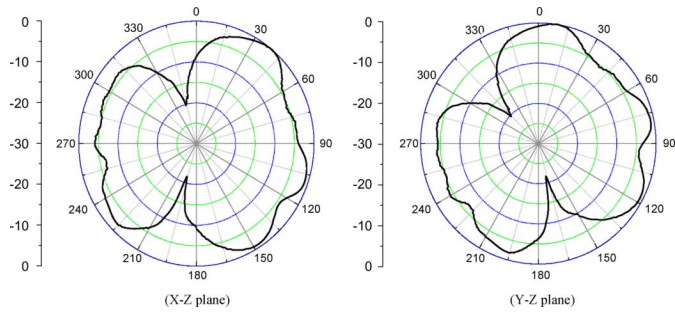


Fig. 4. Radiation patterns at 2.4 GHz.

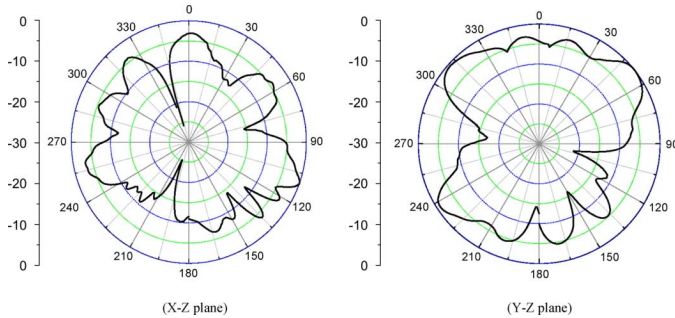


Fig. 5. Radiation patterns at 5.35 GHz.

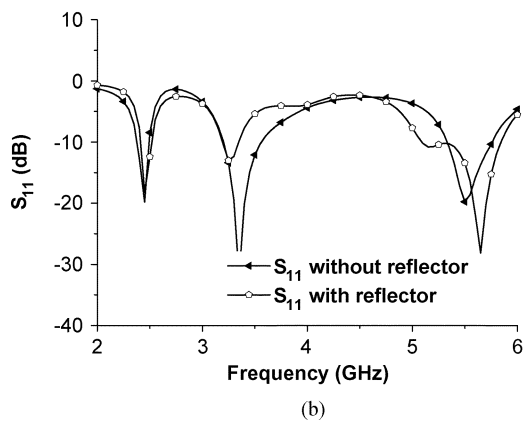
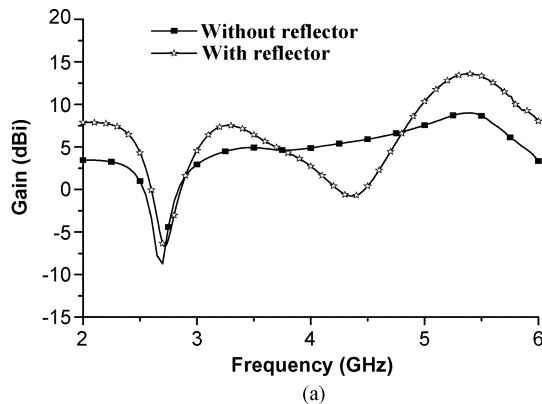


Fig. 6. The effect of the reflector.

plane, while the symmetry of the pattern in this plane is improved at 5.35 GHz through the additional contribution of the higher mode radiated by the rectangular patch. The patterns in  $Y$ - $Z$  plane are approximately symmetric, which are suitable for

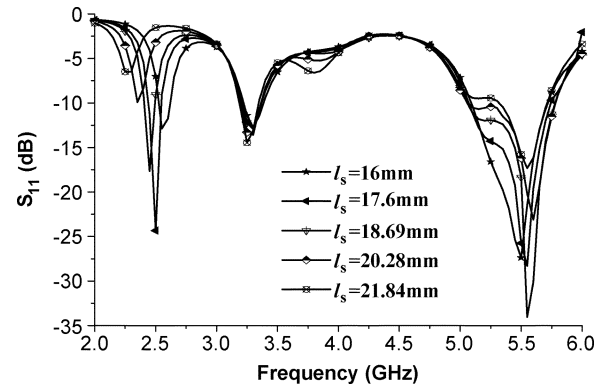
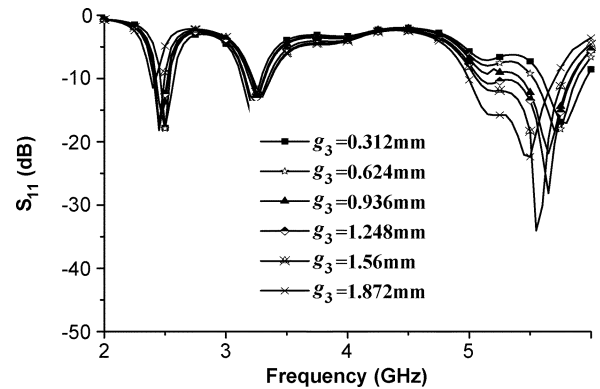


Fig. 7. The return loss of various height of the monopole.

Fig. 8. Effect of horizontal gap  $g_3$  on return loss.

wireless communications. The cross polarizations in the two planes and the two frequency bands are very small according to the results plotted in Fig. 3, and they are not presented here.

A metal reflector was used in the designed antenna as described, so the directivity and the maximum gain values are enhanced in both bands. As is shown in Fig. 6(a), the simulated copolarized gain is increased about an average value of 4 dBi when the reflector was added, while the electrical performance is much less sensitive to fabrication variations. The return loss that is associated with impedance matching is also significantly improved in the two bands through the presence of the reflector, as depicted in Fig. 6(b).

It has to be noted that the presented antenna is sensitive to the geometrical parameters due to the miniaturized ground size. The dominant design parameters are parametrically investigated in Figs. 7–9.

As mentioned above, the fork-like monopole operates at two frequency bands; as a result, when the height  $l_s$  of the monopole is changed, the operating frequency of the two bands will also change. As shown in Fig. 7, when  $l_s$  varies from 16 to 21.84 mm with the other parameters unchanged, the simulated resonant frequency of the lower band decreases from 2.55 to 2.3 GHz almost monotonously, which also can be explained with formulation (1). However, in the higher frequency band, the resonant frequency is decided by the combination of the second resonant frequency of the fork-like monopole and the  $TM_{12}$  higher mode of the rectangular patch, and the frequency shift does not operate so monotonically any more.

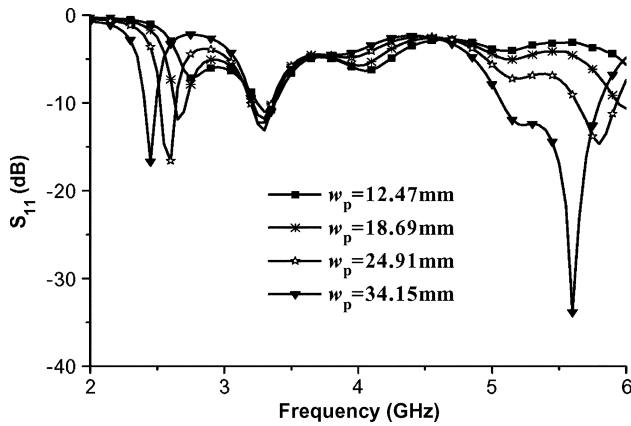


Fig. 9. The effect of width of the rectangular patch.

The vertical gap ( $g_3$ ) between the monopole and the rectangular patch affects the impedance matching of high band dramatically, which is verified with the simulated return losses of different  $g_3$  values shown in Fig. 8. When the gap value is increased with all other parameters fixed, the coupling between the monopole and the patch also changes correspondingly. When  $g_3$  is set to 1.56 mm, the impedance at about 5.5 GHz is matched, and the operating band covers the whole IEEE 802.11a band.

Not only the effect of the fork-like monopole is studied in this letter, as is shown in Fig. 7, but the return loss for different widths of the patch ( $w_p$ ) is also simulated in Fig. 9, with all other parameters unchanged except that the gap  $g_1$  varies correspondingly. It is clear that the resonant frequency of the higher band rises with values of the width  $w_p$  reduced. Since the patch also acts as the impedance matching in the lower frequency band, the change of the patch size clearly affects the low-frequency band, as is shown in Fig. 9.

#### IV. CONCLUSION

A novel single-fed, high-gain, dual-band WLAN antenna is presented in this letter for long-distance communication applications. The frequency bands with return loss below  $-10$  dB cover universally the IEEE 802.11a/b/g standards with maximum gain values of 6.2 and 10.4 dBi in the lower and higher frequency bands, respectively. The dimension of the antenna is slightly larger than other antennas previously reported, but features a significantly higher gain, which is necessary in some applications.

#### REFERENCES

- [1] Y. Cao, C. Lu, and Y. Zhang, "A compact dual band miniaturized antenna for WLAN operation," in *Proc. ICMAT*, Apr. 2008, pp. 416–419.
- [2] Q. He, B. Wang, and J. He, "Wideband and dual-band design of a printed dipole antenna," *IEEE Antennas Wireless Propag. Lett.*, vol. 7, pp. 1–4, 2008.
- [3] R. Li, B. Pan, J. Laskar, and M. M. Tentzeris, "A novel low-profile broadband dual frequency planar antenna for wireless handsets," *IEEE Trans. Antennas Propag.*, vol. 56, no. 4, pp. 1155–1162, Apr. 2008.
- [4] M. N. Suma, R. K. Raj, M. Joseph, P. C. Bybi, and P. Mohanan, "A compact dual band planar branched monopole antenna for DCS/2.4-GHz WLAN applications," *IEEE Microw. Wireless Compon. Lett.*, vol. 16, no. 5, pp. 275–277, May 2006.
- [5] M. J. Kim, C. S. Cho, and J. Kim, "A dual band printed dipole antenna with spiral structure for WLAN application," *IEEE Microw. Wireless Compon. Lett.*, vol. 15, no. 12, pp. 910–912, Dec. 2005.
- [6] L. Boccia, G. Amendola, and G. Di Massa, "A dual frequency microstrip patch antenna for high-precision GPS applications," *IEEE Antennas Wireless Propag. Lett.*, vol. 3, pp. 157–160, 2004.
- [7] R. K. Joshi and A. R. Harish, "A modified bow-tie antenna for dual band applications," *IEEE Antennas Wireless Propag. Lett.*, vol. 6, pp. 468–471, 2007.
- [8] B. S. Izquierdo and J. C. Batchelor, "A dual band belt antenna," in *Proc. iWAT*, 2008, pp. 374–377.
- [9] Y. J. Sung and Y.-S. Kim, "Circular polarised microstrip patch antennas for broadband and dual-band operation," *Electron. Lett.*, vol. 40, no. 9, pp. 520–522, 2004.
- [10] J. Sze, C. Hsu, and S. Hsu, "Design of a compact dual-band annular-ring slot antenna," *IEEE Antennas Wireless Propag. Lett.*, vol. 6, pp. 423–426, 2007.
- [11] B. Li and K. W. Leung, "Dielectric-covered dual-slot antenna for dual band applications," *IEEE Trans. Antennas Propag.*, vol. 55, no. 6, pp. 1768–1773, Jun. 2007.
- [12] Y. Zhou, C. Chen, and J. L. Volakis, "Dual band proximity-fed stacked patch antenna for tri-band GPS applications," *IEEE Trans. Antennas Propag.*, vol. 55, no. 1, pp. 220–223, Jan. 2007.
- [13] M. Wong, A. R. Sebak, and T. A. Denidni, "Analysis of a dual-band dual slot omnidirectional stripline antenna," *IEEE Antennas Wireless Propag. Lett.*, vol. 6, pp. 199–202, 2007.
- [14] W. C. Liu and C. F. Hsu, "Dual-band CPW-fed Y-shaped monopole antenna for PCS/WLAN application," *Electron. Lett.*, vol. 41, no. 7, pp. 390–391, 2005.
- [15] K. Chung, S. Hong, and J. Choi, "Ultrawide-band printed monopole antenna with band-notch filter," *Microw. Antennas Propag.*, vol. 1, no. 2, pp. 518–522, 2007.
- [16] J. T. S. Sumantyo, K. Ito, and M. Takahashi, "Dual-band circularly polarized equilateral triangular-patch array antenna for mobile satellite communications," *IEEE Trans. Antennas Propag.*, vol. 53, no. 11, pp. 3477–3485, Nov. 2005.
- [17] K. Lau, H. Wong, C. Mak, K. Luk, and K. Lee, "A vertical patch antenna for dual-band operation," *IEEE Antennas Wireless Propag. Lett.*, vol. 5, pp. 95–97, 2006.
- [18] H. F. Hammad, Y. M. M. Antar, and A. P. Freundorfer, "Dual band aperture coupled antenna using spur line," *Electron. Lett.*, vol. 33, no. 25, pp. 2088–2090, 1997.
- [19] K. Oh, B. Kim, and J. Choi, "Design of dual and wideband aperture stacked patch antenna with double-sided notches," *Electron. Lett.*, vol. 40, no. 11, pp. 643–645, 2004.